

High-accuracy reconstruction of titanium x-ray emission spectra, including relative intensities, asymmetry and satellites, and *ab initio* determination of shake magnitudes for transition metals

This article has been downloaded from IOPscience. Please scroll down to see the full text article.

2013 J. Phys. B: At. Mol. Opt. Phys. 46 015002

(<http://iopscience.iop.org/0953-4075/46/1/015002>)

View [the table of contents for this issue](#), or go to the [journal homepage](#) for more

Download details:

IP Address: 128.250.144.144

The article was downloaded on 05/08/2013 at 04:22

Please note that [terms and conditions apply](#).

High-accuracy reconstruction of titanium x-ray emission spectra, including relative intensities, asymmetry and satellites, and *ab initio* determination of shake magnitudes for transition metals

C T Chantler¹, J A Lowe¹ and I P Grant²

¹ School of Physics, University of Melbourne, Australia

² Mathematical Institute, Oxford University, Oxford, UK

E-mail: chantler@unimelb.edu.au

Received 12 November 2012, in final form 28 November 2012

Published 17 December 2012

Online at stacks.iop.org/JPhysB/46/015002

Abstract

High resolution x-ray spectroscopy has revealed a complex structure in the spectrum of core-ionized elements. To date, theoretical reproductions must be fitted to experimental results using fitting parameters to account for transition widths, energy corrections, spectator intensities and spectator broadening—up to 12 or more parameters depending on complexity. We provide here the first accurate reconstruction of the $K\alpha$ spectra in titanium using only instrumental broadening widths as free parameters. We also determine structural systematics in observed shake processes in transition metals for the first time.

1. Introduction

The x-ray emission spectrum has long been a subject of interest. Asymmetric peaks and the appearance of satellite features hinted at complex atomic processes beyond a simple bound–bound transition. High-intensity sources such as synchrotrons can provide accurate experimental spectra, however interpretation of this data requires equally accurate theoretical deconvolutions. As well as being of interest for fundamental atomic physics, the shape and relative intensities of peaks are related to the molecular and solid-state environment of the atom [1–4] as well as the means of K-shell vacancy creation (for a comparison of photoionization and electron capture, see e.g. [5]). In this paper the focus is on photoionization of an isolated free atom.

An atom bombarded with electronic or photonic radiation produces ‘characteristic’ radiation [6]. At energies greater than the 1s-ionization threshold (the K edge), the most intense radiation is the $K\alpha$ line, which arises from the $2p \rightarrow 1s$ transition [7]. In heavier elements, relativistic splitting of the 2p shell divides the $K\alpha$ line into distinguishable $K\alpha_1$ and $K\alpha_2$ lines (also often referred to as the KL_2 and KL_3 lines

respectively), arising from the $2p_{3/2} \rightarrow 1s_{1/2}$ and $2p_{1/2} \rightarrow 1s_{1/2}$ transitions respectively. Additional features, known as satellite lines, were also identified in early investigations. Although the correct explanation for these features was offered early on [8], definitive evidence supporting this explanation was not available until computational atomic physics and high-accuracy x-ray experiments [9].

Satellite transitions affect all core-level emission and absorption experiments; satellite features can be seen in ultra-intense x-ray experiments [10], plasma physics experiments [11], x-ray absorption experiments [12] and many others. Despite a long-standing need to understand these transitions, due to the difficulty of atomic structure calculations in complex atoms we have only recently been able to properly investigate these processes theoretically, taking into account such effects as relativity and electron–electron correlation [13, 14].

Following an inner shell ionization event, valence shell electrons experience a change in potential due to the outgoing electron, and due to the increased effective nuclear charge they now experience. The changing potential can cause an additional electron to be excited into a higher shell or the

continuum. These processes are known as shake-up and shake-off respectively. The characteristic radiation emitted by an atom with a shaken-up or shaken-off electron is shifted and distorted compared to the atom without this excitation or ionization. Consequently, a population of core-ionized atoms with a sub-population that has undergone shake-up or shake-off produces a complex x-ray emission spectrum consisting of an overlapping diagram and satellite lines.

A number of authors have published *ab initio* calculations of shake-up/off intensities [15–19]. These values tend to be in good agreement with experimental results for atoms with low atomic number and closed shells. For complex, open-shell atoms, however, these calculations are discrepant from experiment by up to an order of magnitude. For example, Anagnostopoulos found that the 3p satellite contributed 15% to the scandium $K\alpha$ spectrum, compared to Kochur's *ab initio* calculation of 6.0% [17] and Mukoyama's 7.8% [18]. The 3d satellite was found experimentally to contribute 38%, compared to the 5.0% predicted by the two previous sources. At present it is not clear whether the theoretical values or the experimental analysis is at fault [20].

A recent paper by the present authors has provided a new approach to shake-off calculations [21]. Large, relativistic, multi-configuration calculations have been performed for the 3d-transition metal series. These atomic models have been used in a multi-configuration shake-off calculation, and have provided new *ab initio* shake-off intensities which appear to be in better agreement with experiment than anything prior, although some elements still have large discrepancies. Furthermore, the robustness of the experimental analyses to which these theoretical values are being compared is questionable [20].

When the atom is ionized with an energy significantly above the ionization threshold, the outgoing electron leaves the atom in a short time-period compared to the relaxation time of the valence electrons. In this case, the valence electrons experience a sudden change in the internal electromagnetic field due to the reduced screening of the nuclear charge and are affected accordingly, with a finite probability of being excited from their current state [22]. This is called the sudden limit.

It is within this framework of photoionization accompanied by shake processes that x-ray emission spectra are usually analysed [23]. Atomic structure calculations are used to determine the energy and intensities of transitions corresponding to the diagram and satellite cases. These are then broadened and fitted to experimental spectra. From this fitting, satellite intensities can be determined.

An analysis of this sort depends on complex atomic computations. In atoms with multiple open shells (such as transition metals with core and satellite vacancies) these computations are extremely difficult and time-consuming. Presently, only a few transition metals have had such calculations performed [23–25]. Phenomenological methods provide a simple alternative to detailed computations with deceptively plausible results [26, 27]. However, in cases where both phenomenological and theoretical methods have been used the results are inconsistent (cf [23] and [26] for example).

In the following paper we apply the theoretical results of our earlier shake-off calculations [21] to the $K\alpha$ spectra of titanium, consider the extent to which we are able to account for satellite intensities, further consider the robustness of previous fitting methods, and demonstrate a significant reduction in the number of fitting parameters necessary to describe the $K\alpha$ spectrum. We also show that the titanium spectral asymmetry cannot be reproduced using a mixture of valence states as opposed to previous work which showed it was possible for copper [20].

2. Theory

The calculations in this paper were carried out using GRASP2K [28], a fully relativistic, multi-configuration atomic structure package. Two sets of results are referred to in this paper: the first are the shake-off calculations described in detail in [21]. These are *ab initio*, multiconfiguration calculations of the shake-off probabilities. That is to say, they compute the probability that upon ionizing the 1s electron, an additional electron will be ejected into the continuum.

The second are the energy and transition strength calculations described in [24, 13, 14]. These give us line energies, strengths and shapes, allowing diagram and satellite lines to be fit to experimental spectra. The calculations presented in this paper represent a significant advance over our previous work; the total number of configurations involved in this work exceeded 4000 000. These relativistic Dirac CSFs must all be orthogonalized and stable for the computation to converge.

2.1. Atomic structure calculations

Atomic states are expanded into linear combinations of configuration state functions (CSFs) of well defined parity and angular momentum,

$$\Psi(\Pi JM) = \sum_r c_r \Phi(\gamma_r \Pi JM) \quad (1)$$

where $\Phi(\gamma_r \Pi JM)$ are linear combinations of Slater determinants, built from orthonormal Dirac spinors, having parity and angular momentum quantum numbers ΠJM forming an orthonormal basis, and γ_r contains all the quantum numbers necessary to distinguish states. The mixing coefficients, c_r , are determined by diagonalization of the Dirac Hamiltonian, which occurs simultaneously with the optimization of the radial wavefunctions.

A reference CSF set serves as a zeroth order, minimal element basis set. Higher-order corrections are included by increasing the size of the CSF basis. Convergence must be monitored through systematic enlargement of the basis set. The CSF basis was created by allowing single and double excitations from the 3d and 4s subshells to an active set of virtual orbitals. Because the energy ordering of the 3d and 4s subshells differs depending on the core electron configuration, care was taken to exclude CSFs which appeared to be excitations but that actually had a lower energy configuration. Early tests indicated negligible contributions from core-valence excitations which were

subsequently excluded from final calculations in order to improve wavefunction convergence.

Virtual orbitals were optimized independently for each angular momentum + parity symmetry. This results in more rapid convergence and decreases overall computation time, however increases instability especially in higher angular momentum states. Additional large calculations with an expanded number of correlation orbitals were performed on a few of the lower angular momentum + parity symmetries. These have fewer angular momentum couplings available which reduces the size of the calculation, and hence the basis set can be expanded further for these symmetries than for the system as a whole. The rest of the results were then shifted slightly to match the energies thus calculated, improving overall accuracy and providing a better fit to experimental results.

In this paper, we have also expanded our previous calculations to include all possible valence electron distributions between the 3d and 4s shells. The results of this larger calculation will be compared with our previous results later in the paper.

The result of an atomic structure calculation is a series of transition energies and strengths. Since each angular momentum symmetry was calculated individually these need to be renormalized to reflect the branching ratios from the initial states, which are assumed to be populated statistically. An example of these results is presented in figure 2. Each transition is then convolved with a Lorentzian function in order to provide a theoretical spectrum.

2.2. Multiconfiguration shake-off calculations

Prior to ionization, the neutral atom is in an eigenstate of the $N + 1$ electron Hamiltonian, $H(N + 1)$, with an atomic wavefunction $\Psi(N + 1)$. Within the sudden approximation, the removal of an electron occurs adiabatically, and so the atomic wavefunction undergoes the transformation

$$\Psi(N + 1) \rightarrow \Psi^*(N) \quad (2)$$

where $\Psi^*(N)$ is formed by simply removing a core electron from $\Psi(N + 1)$ (the $*$ will be used to denote wavefunctions that are unrelaxed in the ionized Hamiltonian). $\Psi^*(N)$ is no longer an eigenstate of the new atomic Hamiltonian $H(N)$, and can instead be represented as a linear combination of eigenstates

$$|\Psi^*(N)\rangle = \sum_i \langle \Psi(N)^i | \Psi^*(N) \rangle |\Psi(N)^i\rangle \quad (3)$$

where $\Psi(N)^i$ are the eigenstates of $H(N)$. The quantity

$$P = 1 - \langle \Psi(N) | \Psi^*(N) \rangle \quad (4)$$

is the probability for the system, initially in state $|\Psi^*(N)\rangle$, to be discovered in any state other than $|\Psi(N)\rangle$, where both $|\Psi^*(N)\rangle$ and $|\Psi(N)\rangle$ are N electron wavefunctions with the same set of quantum numbers. In other words, P is the probability of either a shake-up or shake-off event occurring.

In the multiconfiguration framework, we can represent the atomic wavefunction as the linear combination of CSFs

(equation (1)). Within this description, the overlap integral in equation (4) becomes

$$\langle \Psi(N) | \Psi^*(N) \rangle = \sum_j \sum_k c_j d_k \langle \Phi(N)_j | \Phi^*(N)_k \rangle \quad (5)$$

where $|\Psi(N)_j\rangle$ and $|\Psi_j^*(N)\rangle$ are the initial and final atomic wavefunctions, c_j and d_k are mixing coefficients, and $|\Phi(N)_j\rangle$ and $|\Phi^*(N)_j\rangle$ are CSFs with parity and total atomic angular momentum equal to that of $|\Psi(N)_j\rangle$.

2.3. Isolating valence configurations

In our previous work [21], shake-off probabilities were averaged over all possible 3d and 4s valence configurations, giving each a statistical weighting. In the present work, we isolate each configuration, in order to individually apply the probabilities to the atomic structure calculations detailed previously.

These results are presented in figure 1. Increasing the occupation of the 3d subshell unsurprisingly increases the probability of an electron being shaken off from that subshell. There are three reasons for this.

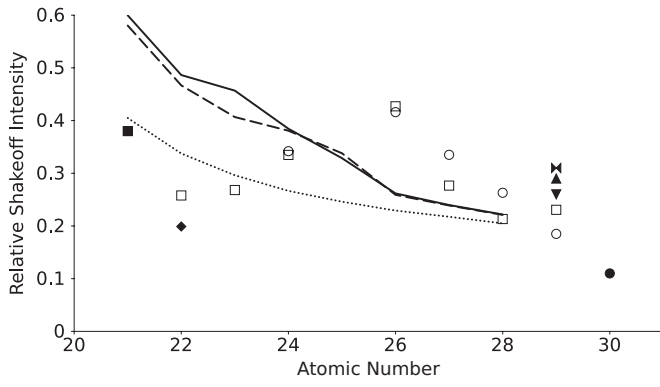
- The probability is on a per-electron basis so increasing the occupation increases the probability of losing an electron.
- Adding electrons to a subshell increases the mean radius for that subshell. Less tightly bound electrons are more likely to be shaken off.
- Additional electrons alter correlation effects. In the first half of the spectrum, adding electrons generally increases correlation effects. In the latter half, adding electrons moves the atom towards a closed shell, and additional electrons have a small effect on correlation.

The overall effect of valence state configuration is greatest in the early transition metals, where there are fewer electrons distributed among the 3d and 4s subshells. In scandium for example, the probability of 3d shake-off ranges from 10% for the $3d^1 4s^2$ configuration to 59% for the $3d^3$ configuration. The empirical value found by Anagnostopoulos *et al* [25] is intermediate at 38%. In the later transition metals, the effect of valence configuration is much less pronounced.

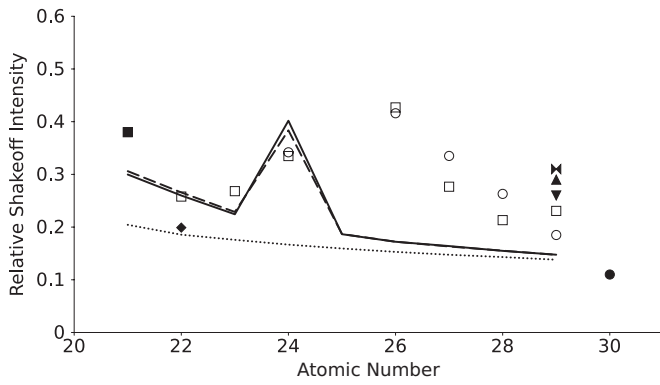
2.4. Fitting

Previously, the results of the atomic structure calculations (section 2.1 and figure 2) would be fit to an experimental spectrum, with each spectator case having a fitted amplitude parameter. In the present work we eliminate the need for such a parameter by making use of the results of section 2.2 (figure 1). *This completely eliminates the need for any fitting of relative transition intensities.* The only fitting parameters are for background removal, transition widths, and in some cases (discussed below) a single overall energy offset where the theoretical results are not in perfect agreement with experiment.

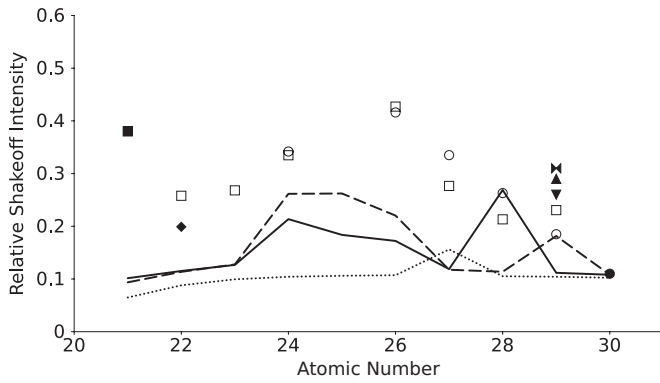
Fitting was carried out using a least-squares algorithm. $K\alpha_1$ and $K\alpha_2$ widths were fit independently. Initially, as in previous work, a single parameter was used to account for



(a) $3d^N$ configuration



(b) $3d^{N-1}4s^1$ configuration



(c) $3d^{N-2}4s^2$ configuration

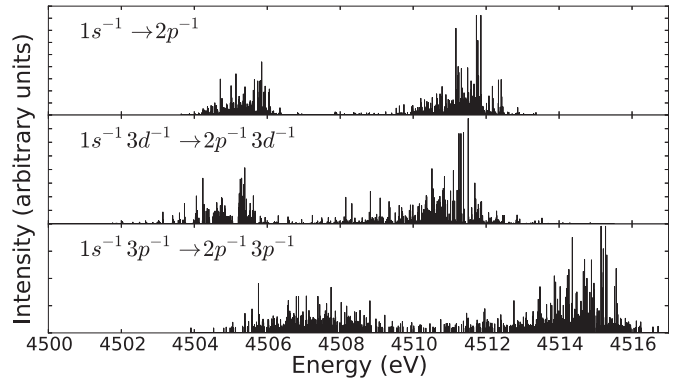
Figure 1. 3d subshell shake-off probabilities for all valence distributions of 3d and 4s electrons in the transition metals. Symbols \blacksquare [25], \blacklozenge [13], \blacktriangleleft [23], \blacktriangle [24], \blacktriangledown [14], \bullet [26], \square [26], \circ [27]. Lines (guide only): \cdots no correlation, $---$ $n = 4$ correlation, $—$ $n = 5$ correlation. Open symbols are phenomenological fits and filled symbols are fits made using atomic structure calculations. The $3d^N$ and $3d^{N-1}4s^1$ series show clear convergence as the basis set is expanded. The $3d^{N-2}4s^2$ series does not appear to have converged in the region $24 < Z < 28$, however, titanium shows little variation with basis set expansion. Phenomenological and multiconfiguration results are discussed in detail in [20].

the additional broadening due to a spectator vacancy, for example,

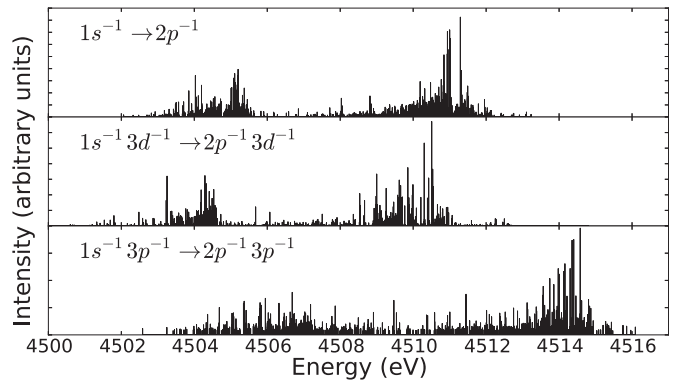
$$\omega_{K\alpha 1+3d} = \omega_{K\alpha 1} + \omega_{3d} \quad (6)$$

$$\omega_{K\alpha 2+3d} = \omega_{K\alpha 2} + \omega_{3d} \quad (7)$$

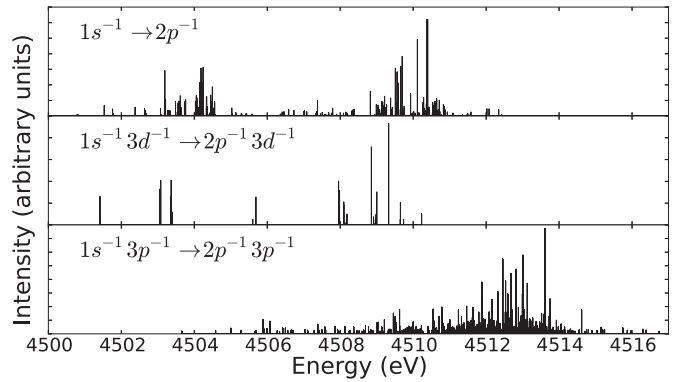
where $\omega_{K\alpha 1}$ is the width of the $K\alpha_1$ transition, $\omega_{K\alpha 1+3d}$ is the width of the $K\alpha_1$ transition with a spectator vacancy



(a) Titanium $3d^4$ configuration



(b) Titanium $3d^3 4s^1$ configuration



(c) Titanium $3d^2 4s^2$ configuration

Figure 2. The results of an atomic structure calculation, as described in section 2.1. These results are for the $K\alpha$ transition in titanium with differing valence electron configurations. The height of the sticks represents the intensity of the transition, with each row normalized in arbitrary units. The relative intensity of the rows is determined using the methods described in 2.2. These transitions are then convolved with Lorentzian broadening prior to fitting. As the number of electrons in the 3d shell increases the possible angular momentum couplings increase dramatically, increasing the density of transitions in the stick figure diagrams.

in subshell 3d, and ω_{3d} is the additional broadening due to the 3d spectator. It was found, however, that the additional broadening parameter ω_{3d} can be eliminated without significantly compromising the goodness of fit. In any case, although this broadening parameter is regularly used in work of this nature, it often takes on unphysical values, as noted previously [13].

Table 1. Titanium fitting parameters for all possible valence configurations. In each case the peak of the spectrum is shifted to align with the experimental spectrum in order to examine which configuration provides the best fit to the spectrum shape. In subsequent columns this shift is removed, as are the additional spectator broadening parameters. All three configurations provide good fits to the spectrum when the peaks are aligned, however, only the $3d^24s^2$ configuration provides a good fit with minimal fitting parameters, with the remaining χ^2_{reduced} dominated by a theoretical peak that is approximately 0.1 eV broader than the experimental peak due to theoretical multiplet spacing.

	Ti $3d^24s^2$			Ti $3d^34s^1$			Ti $3d^4$		
Fixed values									
3p shake-off (%)	7.4	7.4	7.4	6.2	6.2	6.2	5.0	5.0	5.0
3d shake-off (%)	11.5	11.5	11.5	26.0	26.0	26.0	48.6	48.6	48.6
$K\alpha_1$ energy peak (eV)	4510.98	4510.98	4510.98	4511.62	4511.62	4511.62	4512.47	4512.47	4512.47
$K\alpha_2$ energy peak (eV)	4504.90	4504.90	4504.90	4505.71	4505.71	4505.71	4506.35	4506.35	4506.35
Fitted parameters									
$K\alpha_1$ width (eV)	1.79	1.76	1.78	1.86	1.69	1.84	2.07	2.00	3.20
$K\alpha_2$ width (eV)	2.79	2.75	2.75	2.81	2.63	3.06	2.92	2.84	3.48
Δ experimental $K\alpha_1$ (eV)	0.13	0.13	–	–0.49	–0.49	–	–1.23	–1.23	–
Δ experimental $K\alpha_2$ (eV)	0.00	0.00	–	–0.74	–0.74	–	–1.36	–1.36	–
3p spectator broadening (eV)	0.58	–	–	–0.69	–	–	–0.22	–	–
3d spectator broadening (eV)	–0.33	–	–	–0.74	–	–	–1.31	–	–
Derived values									
Total spectra peak $K\alpha_1$ (eV)	4510.77	4510.77	4510.77	4511.02	4511.02	4511.02	4510.89	4510.89	4510.89
Total spectra peak $K\alpha_2$ (eV)	4504.98	4504.98	4504.98	4504.86	4504.86	4504.86	4504.85	4504.85	4504.75
χ^2_{reduced}	4.72	4.91	5.19	1.45	2.26	113.69	1.44	1.84	543.37

3. Results

We considered three possible valence state configurations for titanium: $3d^24s^2$, $3d^34s^1$ and $3d^4$. In fits to experimental spectra, even a slight discrepancy in peak energies can distort the fitted parameters. Therefore, in each case the theoretical spectrum was shifted so that the peaks aligned with the experimental spectra. In calculations of this nature, the relative position of peaks within the spectra converges much faster than the absolute transition energies. While the $3d^24s^2$ transition appears to have converged well on the experimental energy (see [13] for details), at this stage we wish to see which set of transitions provides the best match to the profile *shape*.

The relative intensities of all components, including satellite intensities, were fixed by theory. Thus, the only fitting parameters are individual (instrumental) widths for the $K\alpha_1$ and $K\alpha_2$ transitions, and an additional broadening parameter for each spectator component. Fitting parameters are presented in table 1.

Each of the three valence configuration and satellite intensity combinations can provide very good fits to the experimental spectra. Each fit has significantly different satellite intensities predicted by our shake-off theory. Interestingly, despite this significant difference between valence configurations, in each case our shake-off theory predicts a near-optimal fit. It is not clear what the significance of this is, if any; due to the energy separation of the configurations it is impossible for all three valence configurations to contribute to the spectrum. The only evidence, then, that the nominal $3d^24s^2$ valence configuration is correct is the excellent convergence of the transition energies to within 0.2 eV of the experimental value.

Inspection of table 1 suggests that the broadening of the transition lines due to the spectator vacancy may be negligible. We performed a second set of fittings, in this case removing the two parameters for spectator broadening and setting both to zero. Examination of the χ^2 values for these

fits suggests that with sufficiently accurate calculations, the additional broadening parameters are unnecessary—for any hypothesized valence configuration.

Finally, we remove the energy shift parameters. This of course rules out the $3d^34s^1$ and $3d^4$ configurations, however, the $3d^24s^2$ configuration χ^2 value changes very little. The resulting spectrum and residuals are presented in figure 3. Although the χ^2_{reduced} for this fit is less optimal than some of the other cases considered, this is due to the combination of three small effects: (a) the theoretical spread of the $K\alpha_1$ lines due to multiplet splitting appears to be greater than that observed experimentally by approximately 0.1 eV; (b) the observed 3p satellite intensity (6.2%) is approximately 1 per cent lower than that calculated (7.4%); and (c) the theoretical $K\alpha_1$ peak is 0.13 eV higher than the best-fit peak. Considering that this result uses no fitting parameters besides broadening this is a remarkable agreement between theory and experiment, and the first completely *ab initio* theoretical spectrum that is in good agreement with observation.

We also considered an admixture of states, the results of which are presented in table 2. The improvement in χ^2_{reduced} is minimal, although a combination of the $3d^24s^2$ and $3d^34s^1$ valence configurations is consistent with the experimental results if the theoretical energies are shifted significantly. Importantly, while many might consider our code (or any code) to have inadequacies of eigenvalues at the 0.2 eV level, say, most would expect that such errors would constitute an overall offset and hence that relative shifts of $K\alpha_1$ from $K\alpha_2$ are relatively improbable. We would agree, and this appears to be strong evidence against the significant population of the $3d^34s^1$ valence configuration.

Recent work has shown that the best-fit satellite intensities can be highly sensitive to satellite broadening [20]. In the present work we show that it is possible to present a theoretical spectrum in good agreement with experiment using purely theoretical values, without attempting to determine what is the experimentally observed intensity of the satellite

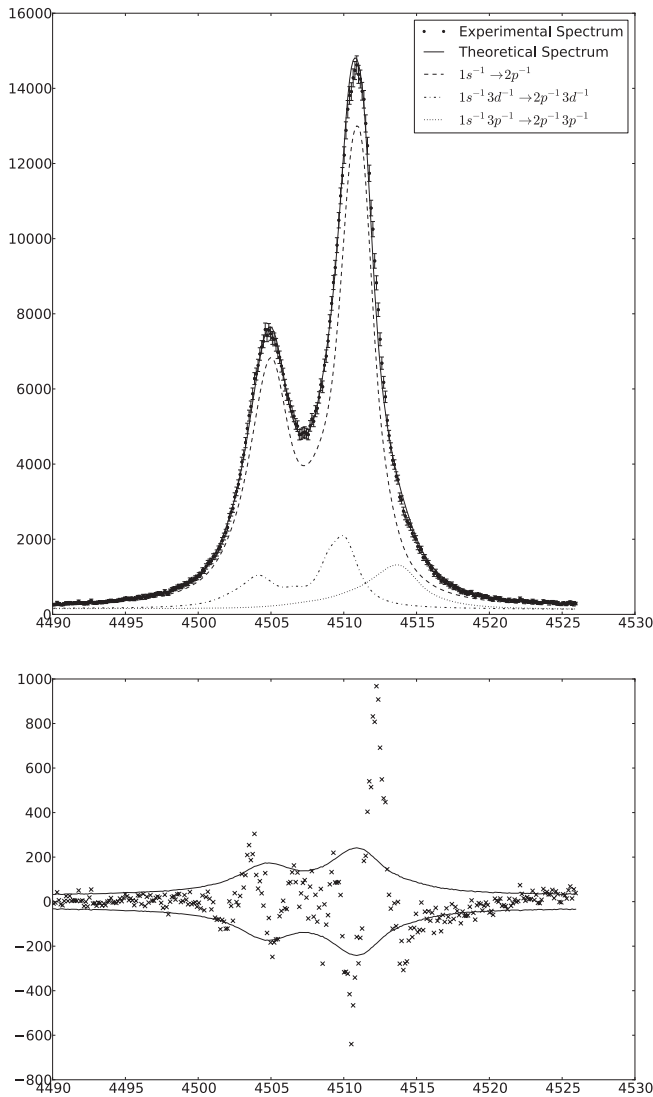


Figure 3. Titanium spectra fitted to experiment [2] with only two fitting parameters ($K\alpha_1$ and $K\alpha_2$ widths). The spectrum fits remarkably well, with all asymmetry accounted for by spectator vacancies. The residuals are mostly contained within experimental uncertainty, with a discrepancy due to a 1 percentage point overestimation of the 3p spectator population, slightly excessive broadening of the $K\alpha_1$ width, and a 0.1 eV offset in the $K\alpha_1$ peak location. This is the first *ab initio* reconstruction of a $K\alpha$ spectrum in agreement with experiment.

Table 2. Fitting parameters for an admixture of the $3d^24s^2$ and $3d^34s^1$ states. When energies are permitted to vary, the mixture of states improves slightly over the $3d^34s^1$ state. When energies are fixed, however, the $3d^24s^2$ state dominates.

Ti $3d^24s^2 + 3d^34s^1$		
Fitted values		
$K\alpha_1$ width (eV)	1.73	1.75
$K\alpha_2$ width (eV)	2.70	2.74
$3d^34s^1$ contribution	59.8%	8.2%
$3d^24s^2$ contribution	40.2%	91.8%
$\Delta_{\text{experimental } K\alpha_1}$	-0.25	-
$\Delta_{\text{experimental } K\alpha_2}$	-0.49	-
χ^2_{reduced}	1.41	4.40

contribution, which depends on assumptions made about broadening parameters. The community clearly needs more accurate spectra in this latter regard.

It is worth emphasizing that in this final fit only two fitting parameters are used (instrumental or total $K\alpha_1$ and $K\alpha_2$ widths). In comparison, our previous work has used six fitting parameters; most prior work has used up to nine or twelve fitting parameters. Since experimental broadening must be accounted for, at least one broadening parameter will always be necessary. For many experimental spectra, a common width is reasonable; for the hole widths, separate broadening widths are clearly needed.

The only remaining theoretical challenge to producing a complete *ab initio* spectrum is to understand the additional broadening of the $K\alpha_2$ peak compared to the $K\alpha_1$. The most likely explanation for this additional broadening is the effect of the Coster–Kronig $L_2 - L_3M_{3,4}$ transition on the $2p_{1/2}^{-1}$ lifetime. This transition is forbidden in free atoms and so atomic calculations of linewidths are unable to account for it. Lifetime widths for the 3d elements that include the Coster–Kronig transition are in better agreement with experimental widths than those that do not [29, 30], however they still differ from experiment by up to 0.5 eV. In solid-state spectra there is also the possibility of nonlifetime contributions such as phonon broadening.

This problem is confounded by the difficulties associated with deconvolving natural broadening from experimental broadening. Furthermore, experimental spectra that are analysed using a single fitted Lorentzian/Voigt function will overestimate the natural linewidth in open-shell systems due to the multiplet structure of the transition [31]. Experimentally reported linewidths in the transition metals are in many cases discrepant by 1 eV or more, such as the widely measured Cu $K\alpha_2$ width [27, 26, 32, 33] which ranges from 2.89 to 4.05 eV. In order to obtain agreement between theory and experiment at the level of the present work, both theoretical and experimental widths would need to be well defined to approximately 0.1 eV accuracy.

4. Conclusion

Using new, high accuracy calculations we have shown that experimental $K\alpha$ spectra can be reconstructed using a fraction of the number of fitting parameters employed previously, and without requiring an arbitrary additional broadening of particular states. This is the first *ab initio* spectra reproduction to do so, and represents a vital step towards complete agreement with experiment. We have shown that the $3d^24s^2$ valence configuration provides good agreement with experiment, however we cannot completely rule out a more complex description. Further improvements in *ab initio* spectra will require accurate theoretical determination of transition widths and careful characterization of experimental and instrumental broadening.

References

- [1] Reinhardt F, Beckhoff B, Eba H, Kanngiesser B, Kolbe M, Mizusawa M, Müller M, Pollakowski B, Sakurai K and Ulm G 2009 Evaluation of high-resolution x-ray absorption and emission spectroscopy for the chemical speciation of binary titanium compounds *Anal. Chem.* **81** 1770–6
- [2] Kawai J, Konishi T, Shimohara A and Gohshi Y 1994 High resolution titanium $K\alpha$ x-ray fluorescence spectra *Spectrochim. Acta B* **49** 725–38
- [3] Raj S, Padhi H C, Basa D K, Polasik M and Pawłowski 1999 $K\beta$ -to- $K\alpha$ x-ray intensity ratio studies on the changes of valence electronic structures of Ti, V, Cr, and Co in their disilicide compounds *Nucl. Instrum. Methods Phys. Res. B* **152** 417–24
- [4] Brunner G, Nagel M, Hartmann E and Arndt E 1982 Chemical sensitivity of the $K\beta/K\alpha$ x-ray intensity ratio for 3D elements *J. Phys. B: At. Mol. Phys.* **15** 4517
- [5] Arndt E, Brunner G and Hartmann E 1982 $K\beta/K\alpha$ intensity ratios for x-ray production in 3D elements by photoionisation and electron capture *J. Phys. B: At. Mol. Phys.* **15** L887
- [6] Barkla C and Sadler C 1908 Homogeneous secondary Rontgen radiations *Phil. Mag.* **16** 550–84
- [7] Moseley H G J 1913 The high-frequency spectra of the elements *Phil. Mag.* **26** 1024–34
- [8] Parratt L G 1936 Excitation potential, relative intensities and wave-lengths of the $K\alpha''$ x-ray satellite line *Phys. Rev.* **49** 502–7
- [9] Deutsch M, Gang O, Hämäläinen K and Kao C C 1996 Onset and near threshold evolution of the Cu K alpha x-ray satellites *Phys. Rev. Lett.* **76** 2424–7
- [10] Young L *et al* 2010 Femtosecond electronic response of atoms to ultra-intense x-rays *Nature* **466** 56–61
- [11] Kritcher A L *et al* 2008 Ultrafast x-ray Thomson scattering of shock-compressed matter *Science* **322** 69–71
- [12] Stern E A 1982 Multielectron contribution to near-edge x-ray absorption *Phys. Rev. Lett.* **49** 1353–6
- [13] Lowe J A, Chantler C T and Grant I P 2010 A new approach to relativistic multi-configuration quantum mechanics in titanium *Phys. Lett. A* **374** 4756–60
- [14] Chantler C T, Lowe J A and Grant I P 2010 Multiconfiguration Dirac Fock calculations in open shell atoms: convergence methods and satellite spectra of copper K alpha photoemission spectrum *Phys. Rev. A* **82** 052505
- [15] Carlson T A, Nestor C W, Tucker T C and Malik F B 1968 Calculation of electron shake-off for elements from $Z = 2$ to 92 with the use of self-consistent-field wave functions *Phys. Rev.* **169** 27–36
- [16] Carlson T A and Nestor C W 1973 Calculation of electron shake-off probabilities as the result of x-ray photoionization of the rare gases *Phys. Rev. A* **8** 2887–94
- [17] Kochur A G, Dudenko A I and Petrini D 2002 Shake process probabilities for outer-shell electrons in atoms with $Z \leq 71$ *J. Phys. B: At. Mol. Opt. Phys.* **35** 395
- [18] Mukoyama T and Taniguchi K 1987 Atomic excitation as the result of inner-shell vacancy production *Phys. Rev. A* **36** 693–8
- [19] Mukoyama T 2005 Electron shake process following inner-shell ionization *X-Ray Spectrom.* **34** 64–8
- [20] Chantler C T, Lowe J A and Grant I P 2012 Anomalous satellite intensity discrepancy in copper x-ray lines *Phys. Rev. A* **85** 032513
- [21] Lowe J A, Chantler C T and Grant I P 2011 *Ab initio* determination of satellite intensities in transition-metal photoemission spectroscopy using a multiconfiguration framework *Phys. Rev. A* **83** 060501
- [22] Krause M O, Vestal M L, Johnston W H and Carlson T A 1964 Readjustment of the neon atom ionized in the K shell by x-rays *Phys. Rev.* **133** A385–90
- [23] Deutsch M, Hölzer G, Härtwig J, Wolf J, Fritsch M and Förster E 1995 $K\alpha$ and $K\beta$ x-ray emission spectra of copper *Phys. Rev. A* **51** 283–96
- [24] Chantler C T, Hayward A C L and Grant I P 2009 Theoretical determination of characteristic x-ray lines and the copper $K\alpha$ spectrum *Phys. Rev. Lett.* **103** 123002
- [25] Anagnostopoulos D F, Sharon R, Gotta D and Deutsch M 1999 $K\alpha$ and $K\beta$ x-ray emission spectra of metallic scandium *Phys. Rev. A* **60** 2018–33
- [26] Ito Y, Tochio T, Oohashi H and Vlaicu A M 2006 Contribution of the (1s3d) shake process to $K\alpha_{1,2}$ spectra in 3D elements *Radiat. Phys. Chem.* **75** 1534–7
- [27] Hölzer G, Fritsch M, Deutsch M, Härtwig J and Förster E 1997 $K\alpha_{1,2}$ and $K\beta_{1,3}$ x-ray emission lines of the 3D transition metals *Phys. Rev. A* **56** 4554–68
- [28] Jonsson P, He X, Froese-Fischer C and Grant I P 2007 The grasp2K relativistic atomic structure package *Comput. Phys. Commun.* **177** 597–622
- [29] Yin L I, Adler I, Chen M H and Crasemann B 1973 Width of atomic L_2 and L_3 vacancy states near $Z = 30$ *Phys. Rev. A* **7** 897–903
- [30] Campbell J L and Papp T 2001 Widths of the atomic KN7 levels *At. Data Nucl. Data Tables* **77** 1–56
- [31] Kučas S, Karazija R and Kynienė A 2006 On the determination of natural width of levels for the open shell atoms with inner vacancy *J. Phys. B: At. Mol. Opt. Phys.* **39** 1711–9
- [32] Maskil N and Deutsch M 1988 Structure and wavelength of the Cu $K\alpha_2$ x-ray emission line *Phys. Rev. A* **37** 2947–52
- [33] Citrin P H, Eisenberger P M, Marra W C, Åberg T, Utriainen J and Källne E 1974 Linewidths in x-ray photoemission and x-ray emission spectroscopies: what do they measure? *Phys. Rev. B* **10** 1762–5